Jeffrey D. Price, Chie Hotta-Iwamura, Yongge Zhao, Nicole M. Beauchamp, and Kristin V. Tarbell

DCIR2$^+$ cDC2 DCs and Zbtb32 Restore CD4$^+$ T-Cell Tolerance and Inhibit Diabetes

Diabetes 2015;64:3521–3531 | DOI: 10.2337/db14-1880

During autoimmunity, the normal ability of dendritic cells (DCs) to induce T-cell tolerance is disrupted; therefore, autoimmune disease therapies based on cell types and molecular pathways that elicit tolerance in the steady state may not be effective. To determine which DC subsets induce tolerance in the context of chronic autoimmunity, we used chimeric antibodies specific for DC inhibitory receptor 2 (DCIR2) or DEC-205 to target self-antigen to CD11b$^+$ (cDC2) DCs and CD8$^+$ (cDC1) DCs, respectively, in autoimmune-prone nonobese diabetic (NOD) mice. Antigen presentation by DCIR2$^+$ DCs but not DEC-205$^+$ DCs elicited tolerogenic CD4$^+$ T-cell responses in NOD mice. β-Cell antigen delivered to DCIR2$^+$ DCs delayed diabetes induction and induced increased T-cell apoptosis without interferon-γ (IFN-γ) or sustained expansion of autoreactive CD4$^+$ T cells. These divergent responses were preceded by differential gene expression in T cells early after in vivo stimulation. *Zbtb32* was higher in T cells stimulated with DCIR2$^+$ DCs, and overexpression of Zbtb32 in T cells inhibited diabetes development, T-cell expansion, and IFN-γ production. Therefore, we have identified DCIR2$^+$ DCs as capable of inducing antigen-specific tolerance in the face of ongoing autoimmunity and have also identified Zbtb32 as a suppressive transcription factor that controls T cell–mediated autoimmunity.

Antigen-specific induction of T-cell tolerance is a desired therapeutic outcome for type 1 diabetes because of the potential to stop undesirable pathogenic responses while minimizing nonspecific immune inhibition. To date, little clinical efficacy has been observed for this approach (1,2). Autoimmune individuals elicit immune responses in an inflammatory context and are therefore refractory to tolerance induction, yet most studies of T-cell tolerance have been performed in either a steady-state context or in models of autoimmunity requiring immunization with autoantigen that best model the effector phase (3). Therefore, to move beyond therapies that nonspecifically block effector functions, it is important to learn what conditions are needed to enable antigen-specific T-cell tolerance induction in a chronic inflammatory autoimmune environment, which can be modeled using autoimmune-prone nonobese diabetic (NOD) mice that show spontaneous loss of self-tolerance due to genetic and environmental factors (4).

These factors leading to autoimmune diabetes alter the capacity of antigen-presenting cell populations to induce tolerance (5). In NOD mice, dendritic cells (DCs) are in the pancreas prior to T-cell infiltration and are important for diabetes pathogenesis and regulation (6–8). DCs are central for both induction of immunity and tolerance (9), and conventional DCs (cDCs) can be divided into two broad subsets with similar function in both mouse and human (10). The cross-presenting cDC1 express XCR1 in both human and mouse and can be identified by CD8 or CD103 expression in mice (11,12). cDC2 are CD11b$^+$ in both mouse and human, CD1c$^+$ in human, and DC inhibitory receptor 2 (DCIR2)$^+$ in mice (10). CD11b$^+$ cDC2 are strong stimulators of antibody production and CD4$^+$ effector T-cell (Teff) responses and induce regulatory T-cell (Treg) proliferation, whereas CD8$^+$ cDC1 endocytose

Immune Tolerance Section, Diabetes, Endocrinology, and Obesity Branch, National Institute of Diabetes and Digestive and Kidney Diseases, National Institutes of Health, Bethesda, MD

Corresponding author: Kristin V. Tarbell, tarbellk@niddk.nih.gov.

Received 10 December 2014 and accepted 5 June 2015.

This article contains Supplementary Data online at http://diabetes.diabetesjournals.org/lookup/suppl/doi:10.2337/db14-1880/-/DC1.

J.D.P. and C.H.-I. contributed equally to this work.

J.D.P. is currently affiliated with the Nebraska Center for Virology, University of Nebraska-Lincoln, Lincoln, NE.

apoptotic blebs and can result in T-cell tolerance directed against self-antigens (13,14). cDC1 are dependent on the transcription factor Batf3, and loss of Batf3 in NOD mice leads to a block in diabetes pathogenesis (12,15).

Patients with type 1 diabetes and NOD mice carry diabetes susceptibility alleles, some of which affect antigen-presenting cells, such as DCs, that lead to a loss of tolerance and development of autoimmune diabetes (16). The normal generation and maintenance of DCs may be altered in autoimmune diabetes and affect T-cell tolerance induction (17–19). T cells appear in the pancreas of NOD mice as early as 4 weeks of age, but hyperglycemia does not occur until 12 weeks or later. This can be modeled by $CD4^+$ autoreactive BDC2.5 T-cell receptor (TCR) transgenic T cells that respond to the β-cell granule protein chromogranin A as well as a series of mimetope peptides (20–22). Prediabetic mice and humans show islet-specific T cells and antibody responses indicating active autoimmunity, but simultaneous immune regulation can slow β-cell destruction (23–25). Unlike some autoimmune diseases, the early phases of autoimmune diabetes are clinically silent because sufficient β-cell destruction for hyperglycemia does not occur until late. Autoantibodies and MRI signal present in prediabetic mice and humans correlate with immune infiltrate in the pancreatic islets (26,27), and individuals with high risk can now be identified prior to hyperglycemia (28). Therefore, this prediabetic phase represents ongoing autoimmunity and is of interest as a target of immunotherapy.

Targeting antigen to DCs without adjuvant can induce T-cell tolerance (29–31). Chimeric antibodies against lectin antigen-uptake receptors efficiently target antigen to specific DC subsets, including DCIR2 expressed by $CD11b^+$ cDC2 and DEC-205 expressed by $CD8^+$ cDC1 and some migratory DCs (32). This allows characterization of in vivo presentation of relevant antigens by specific DC subsets and has therapeutic potential for induction of both immunity and tolerance (33). Interestingly, in mice without spontaneous autoimmunity, DEC-205^+ migratory DCs are important for tolerance via Treg induction (34). Antigen delivered to $CD11b^+$ DCs via anti-DCIR2 can also be tolerogenic in non–autoimmune-prone mice, but little is known about the differential programs these DC subsets elicit in $CD4^+$ T cells (31,35).

In contrast to these findings of DC-mediated tolerance induction, we have shown, surprisingly, that DEC-205^+ cDC1 are unable to induce $CD4^+$ T-cell tolerance in NOD mice (18). In this autoimmune context, DEC-205^+ DCs elicit expansion and effector function, even when starting with naïve T cells. Nontargeted antigen delivery will likely have to overcome this effector response to induce tolerance.

Therefore, we now asked if other DC subpopulations could elicit a more tolerogenic response from autoreactive $CD4^+$ T cells in NOD mice. Comparing T cells stimulated by DC subpopulations divergent in tolerogenic ability allows identification of pathways critical for tolerance induction in this context. Here, we demonstrate that delivery of antigen to $DCIR2^+$ DCs in NOD mice induces a tolerant phenotype in diabetogenic BDC2.5 $CD4^+$ T cells and inhibits diabetes development in a NOD.*scid* transfer system. T cells stimulated by $DCIR2^+$ DCs do not produce interferon-γ (IFN-γ) and undergo significant deletion. Early after stimulation with $DCIR2^+$ DCs, T cells displayed distinct gene expression, including higher levels of zinc finger and BTB domain containing 32 (*Zbtb32*), a transcription factor that can inhibit T-cell differentiation (36). We found that overexpression of Zbtb32 in BDC2.5 T cells increases deletion and inhibits their ability to induce diabetes. These results demonstrate that although DC-mediated tolerance is impaired in the context of chronic autoimmunity, specific DC subsets such as $DCIR2^+$ DCs can still elicit diabetes-inhibiting T-cell responses, in part by increased expression of Zbtb32.

RESEARCH DESIGN AND METHODS

Mice

Original breeding pairs of NOD, NOD.BDC2.5, NOD.Thy1.1, NOD.*scid*, and C57Bl/6 mice were obtained from The Jackson Laboratory (Bar Harbor, ME). NOD.BDC2.5. FoxP3-green fluorescent protein (GFP) mice were a gift of Vijay Kuchroo (Harvard University). Six- to eleven-week-old mice were used. All mice were bred and housed under specific pathogen-free conditions at the National Institutes of Health according to protocols approved by the Institutional Animal Care and Use Committee.

Antibodies and Flow Cytometry

FoxP3 (FJK-16s)-APC antibodies were purchased from eBioscience (San Diego, CA). CD40 (3/23)-FITC and IFN-γ (XMG1.2)-APC antibodies were purchased from Becton Dickinson (San Jose, CA). CD4 (GK1.5)-PacBlue, Thy1.1 (OX7)-APC, Thy1.1-PerCP, Thy1.2 (30-H12)-APC, Thy1.2-PerCP, interleukin (IL)-2 (JES6–5H4)-Alexa488, CD11c (N418)-PerCP, CD11b (M1/70)-PE, IL-3 (MP2–8F8)-PE, and CD8 (53–6.7)-PacificBlue were purchased from BioLegend (San Diego, CA). Viability was assessed by Live/Dead Fixable Aqua staining (Life Technologies, Grand Island, NY). All DC stains were done in the presence of TruStain FcX (BioLegend). Flow cytometry was performed on a CyAn (Beckman Coulter, Brea, CA) or LSR II (Becton Dickinson). Western blotting was performed using Flag (F3165) and β-actin (A1978) antibodies (Sigma-Aldrich, St. Louis, MO) and the Amersham ECL Western Blotting Kit (GE Healthcare Bio-Sciences, Pittsburgh, PA) as their detection reagent.

Production of Chimeric Antibodies

αDEC-205 and αDCIR2 antibodies generated from their original hybridomas (NLDC-145 and 33D1, respectively) were obtained from Ralph Steinman and Michel Nussenzweig (The Rockefeller University). Antibodies contain an altered IgG1 heavy chain constant region that ablates binding by Fc receptors (37), followed by a linker sequence and the antigenic peptides. αDEC-BDC and

αDCIR2-BDC (BDC2.5 mimotope 1040-55) (20) were expressed and purified as previously reported (18,29). Antibody binding to CHO lines expressing DEC-205 or DCIR2 (Juliana Idoyaga, Steinman Laboratory, The Rockefeller University) was analyzed using a polyclonal goat anti-mouse IgG-PE (Jackson ImmunoResearch, West Grove, PA), and binding to spleen DCs was analyzed by an anti-mouse IgG1-Alexa488 (Life Technologies). All batches were tested for functional activity by BDC2.5 T-cell proliferation in vivo and assessed for low endotoxin levels (<0.2 EU/mL) by LAL assay (Lonza, Basel, Switzerland).

Purification and Stimulation of T Cells

$CD4^+$ T cells were recovered from spleens of NOD.BDC2.5 mice by negative selection as previously reported (18). T cells were labeled with 5 μmol/L carboxyfluorescein succinimidyl ester (Life Technologies), and $1–2 \times 10^6$ cells were injected intravenously. One day after T-cell injection, 100 ng of chimeric antibodies or controls was injected intraperitoneally, unless otherwise indicated.

Regulation of Diabetes by DC-Targeting Antibodies

$CD4^+CD25^-$ BDC2.5 T cells were isolated from spleen by negative selection as above, with the addition of biotinylated αCD25 (BioLegend). T cells (5×10^4) were injected intravenously into NOD.*scid* mice. These NOD.*scid* mice were treated 1 day prior, and concurrently with T cells, with either PBS or 500 ng αDEC-BDC or αDCIR2-BDC. Mice were considered diabetic on the first day of two consecutive days with blood glucose levels over 250 mg/dL.

Cytokine Production and Apoptosis

Lymphoid cells were stimulated and intracellular cytokine staining was performed as previously described (18). Total cell numbers in lymphoid tissues were counted by gathering the total number of BDC2.5 T cells within the flow sample and the percentage of the total cell count in the tissue assessed by trypan blue exclusion. For apoptosis measurement, lymphoid cells stimulated for 4 days in vivo were examined by CD4 and Thy1 antibodies followed by a 1-h incubation with Mito Casp reagents (Cell Technology, Inc., Mountain View, CA) and immediate detection by FACS analysis.

Sorting of Treg and Teff

$CD4^+$ T cells were purified as described from spleens of BDC2.5.FoxP3-GFP mice. Cells were then stained for CD4 and sorted on a BD FACSAria for $CD4^+GFP^+$ (Treg) and $CD4^+GFP^-$ (Teff) populations. Cells were then transferred intravenously into NOD.Thy1.1 mice as previously described.

T-Cell Rechallenge

Transferred BDC2.5 $CD4^+$ T cells were stimulated for 10 days with PBS or 100 ng αDCIR2-BDC, followed by challenge by PBS or 100 ng αDCIR2-BDC with 20 μg αCD40 plus 50 μg polyinosinic-polycytidylic acid [poly(I:C)] plus 5 μg lipopolysaccharide (LPS). Spleen and lymph nodes were collected after 4 days and BDC2.5 T-cell numbers were assessed by flow cytometry.

Gene Expression Analysis

BDC2.5.Thy1.1 T cells were purified, transferred to NOD mice, and stimulated with chimeric antibodies as described. Fourteen hours after injection of αDEC-BDC or αDCIR2-BDC, BDC2.5 T cells were sorted from spleen and lymph nodes by Thy1.1 positivity on a BD FACSAria. RNA was isolated by the PicoPure kit (Life Technologies) according to the manufacturer's instructions. RNA amount and quality were checked by Bioanalyzer analysis. RNA was provided to the National Institute of Diabetes and Digestive and Kidney Diseases (NIDDK) Genomics Core for cDNA synthesis and array analysis. Gene expression was interrogated using Mouse Gene 1.0 ST arrays (Affymetrix, Santa Clara, CA), followed by analysis by Partek Genomics Suite. The array data have been deposited in the National Center for Biotechnology Information Gene Expression Omnibus under accession number GSE69554 (http://www.ncbi.nlm.nih.gov/geo/query/acc.cgi?acc=GSE69554). The mRNA levels of *Il2*, *Il3*, *Irf1*, and *Zbtb32* were quantitatively confirmed using NanoString nCounter analysis.

Transfection of BDC2.5 T Cells and Diabetes Transfer

$CD4^+$ BDC2.5 T cells were isolated from spleen and lymph nodes of 6- to 12-week-old NOD.BDC2.5 mice using the $CD4^+$ T-cell isolation kit (Miltenyi) and transfected with either the pcDNA3.1 plasmid or *Zbtb32* plasmid using the Amaxa Nucleofection kit for mouse T cells (Lonza). Transfected cntrl-BDC2.5 T cells (5×10^5) or Zbtb32-BDC2.5 T cells (5×10^5) were injected intravenously into 6-week-old NOD.*scid* mice. The incidence of diabetes was monitored as described. Cell viability after transfection was measured by FACS, and transfected Zbtb32 expression was determined by Western blotting.

Insulitis Score

Pancreata from treated NOD.*scid* mice were fixed in formalin. Paraffin-embedded tissues were sectioned and stained with hematoxylin-eosin. The degree of insulitis was scored in a blinded fashion using the following scale: 0 = intact islet, 1 = peri-insulitis, 2 = moderate insulitis (<50% of the islet infiltrated), 3 = severe insulitis (≥50% of the islet infiltrated), and 4 = destructive insulitis. At least 20 islets per pancreas were analyzed by two independent examiners.

Statistics

Differences between groups in diabetes experiments (Figs. 1*A* and 8*E*) were analyzed by the log-rank test. Analysis of all other data was done using an ANOVA analysis with Bonferroni posttests or an unpaired, two-tailed Student *t* test with 95% CI (GraphPad Prism, San Diego, CA). *P* values <0.05 were considered significant.

RESULTS

To study DC-mediated tolerance induction in autoimmune NOD mice, we generated chimeric antibodies that target a BDC2.5-stimulatory mimetope peptide to antibodies against the lectin DEC-205 (αDEC-BDC) or DCIR2 (αDCIR2-BDC) found on cDC1 $CD8^+$ and cDC2 $CD11b^+$

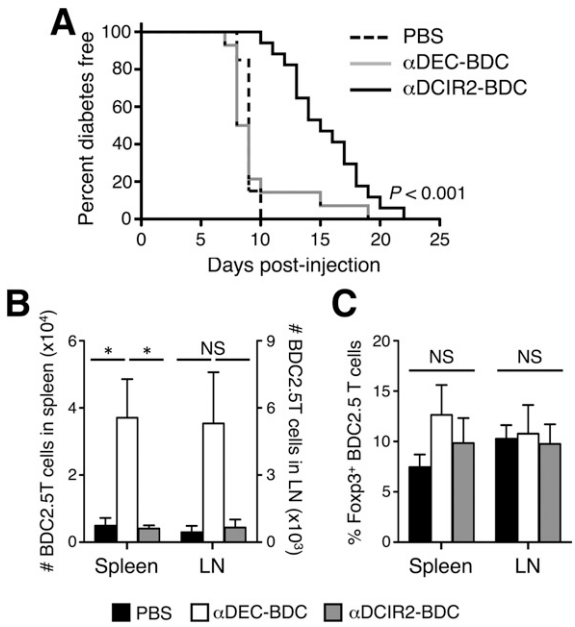

Figure 1—Stimulation of BDC2.5 T cells by DCIR2$^+$ DCs delays diabetes development in NOD.*scid* mice. *A*: Percent of NOD.*scid* mice that are diabetes free after injection with CD4$^+$CD25$^-$ BDC2.5 T cells and the indicated treatments. Statistical analysis was performed with log-rank test. $P < 0.001$ for αDEC-BDC vs. αDCIR2-BDC; $P = 0.452$ for PBS vs. αDEC-BDC. Summation of four experiments. $n = 28$ mice treated with PBS, $n = 20$ mice treated with αDEC-BDC, and $n = 19$ mice treated with αDCIR2-BDC. BDC2.5 T cells (5×10^4) were transferred to NOD.*scid* mice and treated with the indicated conditions. Graphs indicate the total BDC2.5 T-cell number (*B*) and the ratio of Foxp3$^+$ BDC2.5 T cells (*C*) in NOD.*scid* mice on day 5. Average of three independent experiments ± SEM. Statistical analysis was performed with one-way ANOVA with Bonferroni posttest. *$P < 0.05$. LN, lymph nodes; NS, not significant.

DCs, respectively (Supplementary Fig. 1*A* and *B*). These antibodies specifically bind to their target lectins (Supplementary Fig. 1*B*), and they functionally targeted antigenic peptide to DCs for efficient stimulation of β-cell–reactive BDC2.5 T cells in vivo, whereas the same dose of antigen given via a nonspecific antibody did not significantly stimulate BDC2.5 T cells (18).

To determine how autoantigen presentation by DEC-205$^+$ or DCIR2$^+$ DCs affected diabetes pathogenesis, CD4$^+$CD25$^-$ T cells from NOD.BDC2.5 mice were injected into NOD.*scid* mice to induce diabetes. The NOD.*scid* mice were treated with PBS, αDEC-BDC, or αDCIR2-BDC and followed for hyperglycemia. αDEC-BDC did not alter the time to diabetes, as previously reported (18,38) (Fig. 1*A*). αDCIR2-BDC, on the other hand, significantly delayed diabetes progression as compared with PBS or αDEC-BDC ($P < 0.001$ for each) (Fig. 1). Next, T-cell expansion and Treg induction were measured at day 5 in NOD.*scid* mice transferred with BDC2.5 T cells. The net expansion of islet-specific cells was significantly higher in mice given αDEC-BDC (Fig. 1*B*), but no differences in the proportion of Foxp3$^+$ cells were observed (Fig. 1*C*), suggesting that the differential diabetes induction was not due to changes in Treg levels but perhaps due to differences in proliferation or cell death. Therefore, these two DC subsets induce distinct pathogenic outcomes in autoreactive T cells.

To understand the differential effects of antigen presentation by these two subsets, BDC2.5 T-cell responses were examined in lymphoreplete NOD mice. Because initial TCR engagement and subsequent CD69 upregulation are necessary for antigen-specific T-cell activation or tolerance induction (39), early T-cell responses after in vivo DC stimulation were measured. Treatment with a dose range from 10 ng to 1 μg of αDEC-BDC and αDCIR2-BDC led to an increase of T-cell activation markers after 24 h of stimulation with DEC-205$^+$ or DCIR2$^+$ DCs (Fig. 2*A*). Activation was observed at a low dose of chimeric antibody, indicating that the targeting of the antigenic peptide was highly efficient. As expected due to the greater presence of DEC-205$^+$ DCs in lymph nodes and DCIR2$^+$ DCs in spleen (31), the activation of BDC2.5 T cells was more efficient for αDCIR2-BDC in spleen and more efficient for αDEC-BDC in lymph nodes (Fig. 2*A*). Antigen targeted to either DEC-205$^+$ or DCIR2$^+$ DCs induced proliferation and initial expansion in BDC2.5 T cells in both the spleen and in lymph nodes after 3 days of stimulation (Fig. 2*B* and *C*). After 10 days of stimulation, cells continued proliferating when stimulated by αDEC-BDC (Fig. 2*B*). However, a significant decrease in the number of BDC2.5 T cells was observed in spleen and lymph nodes at day 10 after stimulation with αDCIR2-BDC as compared with αDEC-BDC (Fig. 2*C*). Cell numbers after 10 days of stimulation by αDCIR2-BDC were similar to the number of cells remaining in mice given no antigenic stimulation (PBS). Thus, whereas αDEC-BDC induced proliferative responses that led to cell accumulation, αDCIR2-BDC induced initial proliferation that was followed by contraction of the T-cell population in lymphoid tissues.

Because autoimmune pathogenesis in NOD mice is associated with a T-helper type 1 response (40), we examined the cytokines that are secreted after stimulation by αDEC-BDC or αDCIR2-BDC. As we previously observed (18), stimulation with αDEC-BDC led to secretion of IL-2 and IFN-γ by BDC2.5 T cells at both day 3 and day 10 (Fig. 3). Stimulation with αDCIR2-BDC, however, led to increased IL-2 secretion by BDC2.5 T cells in the spleen at day 3, but not in the remaining T cells at day 10, and did not induce IFN-γ secretion at any time point tested (Fig. 3). IL-4, IL-10, and IL-17 were not observed after stimulation with either DC subset (data not shown). Therefore, antigen delivered to DEC-205$^+$ DCs, but not DCIR2$^+$ DCs, induces sustained expansion and effector responses in NOD mice.

Tolerance can be broken by maturation of DC populations, and mature DEC-205$^+$ and DCIR2$^+$ DCs will stimulate effector T cells rather than tolerance (29,31). NOD CD8$^+$ DCs express higher CD40 compared with C57Bl/6 mice, and blocking this pathway abrogated expansion of BDC2.5 T cells after stimulation with DEC-205$^+$ DCs, suggesting that increased CD40 may contribute to the inability of NOD CD8$^+$ DCs to induce tolerance

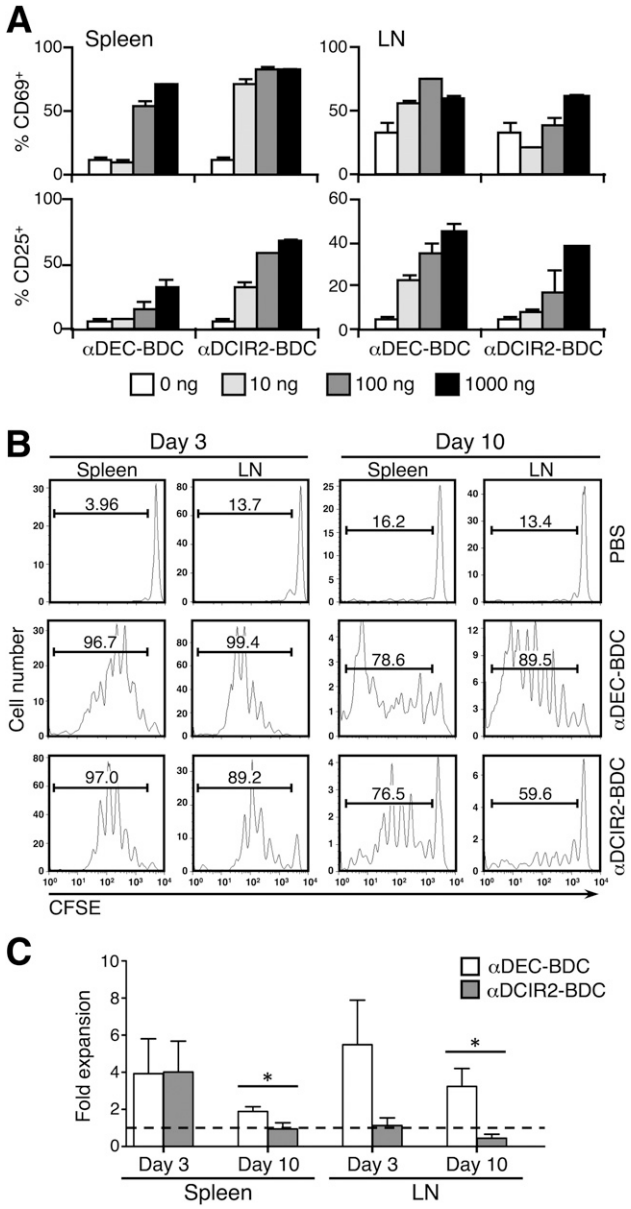

Figure 2—DEC-205$^+$ DCs, but not DCIR2$^+$ DCs, elicit sustained expansion of BDC2.5 T cells in NOD mice. *A*: Activation markers (CD69 and CD25) on BDC2.5 T cells in spleen and lymph nodes (LNs) after stimulation of BDC2.5 T cells in NOD mice with the indicated dose of αDEC-BDC or αDCIR2-BDC (or PBS control, 0 ng). Average of two independent experiments ± SEM. *B*: Histograms of carboxyfluorescein succinimidyl ester (CFSE) dilution for BDC2.5 T cells stimulated with the indicated antibodies at day 3 or day 10. Numbers indicate the percentage of divided T cells. *C*: Fold expansion (over PBS controls, dotted line at fold expansion 1) of BDC2.5 T cells after the indicated treatments. Statistical analysis was performed with one-way ANOVA with Bonferroni posttests. *$P < 0.05$ for αDEC-BDC vs. αDCIR2-BDC.

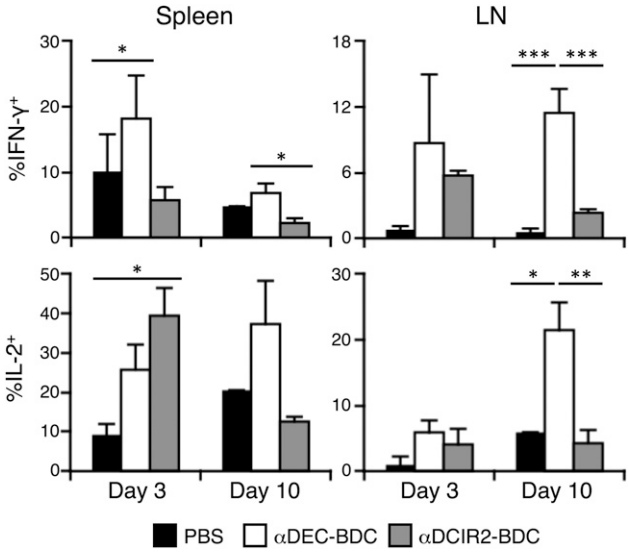

Figure 3—DEC-205$^+$ DCs, but not DCIR2$^+$ DCs, stimulate sustained IL-2 and IFN-γ production by T cells. Percent of BDC2.5 T cells expressing IL-2 or IFN-γ after the indicated treatments for 3 or 10 days in NOD mice after the indicated treatments. Average of four independent experiments ± SEM. Statistical analysis was performed with one-way ANOVA with Bonferroni posttests. *$P < 0.05$; **$P < 0.01$; ***$P < 0.001$. LN, lymph nodes.

(18). Therefore, we measured the level of CD40 expression on CD8$^+$ and CD11b$^+$ DCs. CD40 expression was higher on CD11b$^+$ DCs from NOD mice compared with C57Bl/6 mice, consistent with the ongoing autoimmunity in prediabetic NOD mice. But CD11b$^+$ DCs from both strains expressed lower CD40 levels than CD8$^+$ DCs (Fig. 4). This lower CD40 expression on CD11b$^+$ DCs could contribute to their lower immunogenicity in NOD mice.

To rule out the possibility that the reduction in T cells after treatment with αDCIR2-BDC was due to increased trafficking to sites of endogenous antigen after stimulation, the number of T cells in the pancreatic-draining lymph node was measured. As expected for β-cell–specific T cells, some proliferation of BDC2.5 T cells could be observed in pancreas-draining lymph nodes, even without exogenous stimulation (Supplementary Fig. 2*A*). BDC2.5 T-cell numbers in the pancreatic-draining lymph nodes were similar after stimulation by DCIR2$^+$ or DEC-205$^+$ DCs (Supplementary Fig. 2*B*). Therefore, the T-cell reduction in spleen and peripheral lymph nodes after αDCIR2-BDC stimulation is not due to migration of the T cells to sites of endogenous antigen presentation.

DEC-205$^+$ and DCIR2$^+$ DC subsets have been reported to be important for Treg induction or expansion, respectively (34,41). To separately test induction or expansion of Tregs, GFP$^+$ (Foxp3$^+$) and GFP$^-$ CD4$^+$ cells were sorted from NOD.BDC.Foxp3-GFP mice and injected into NOD mice along with DC-targeted antigen (Fig. 5*A*). Although αDEC-BDC and αDCIR2-BDC both caused proliferation and expansion of injected Foxp3$^+$ Tregs at day 3, the expansion elicited by the two DC subsets was not significantly different, and this expansion was similar to the expansion of GFP$^-$ cells (Fig. 5*B* and *C*). Likewise, little conversion of GFP$^-$ to GFP$^+$ cells was observed after stimulation by either DC subset (Fig. 5*C*). No significant increase in the percentage of Foxp3$^+$ BDC2.5 T cells after stimulation of total CD4$^+$ BDC2.5 T cells by DEC-205$^+$ or DCIR2$^+$ DCs was observed at antibody doses

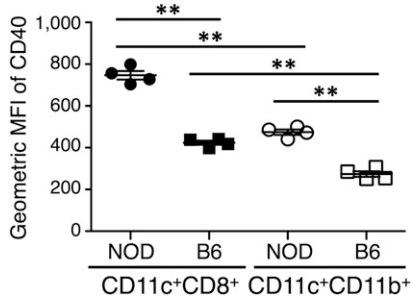

Figure 4—NOD $CD8^+$ DCs express higher levels of CD40 than $CD11b^+$ DCs. Geometric mean fluorescence intensity (MFI) of CD40 on spleen $CD8^+$ or $CD11b^+$ DCs in C57Bl/6 (B6) or NOD mice. Each dot represents a single mouse, representative of three independent experiments. Statistical analysis was performed with two-way ANOVA with Bonferroni posttests. $^{**}P < 0.0001$.

ranging from 10 to 1,000 ng (Fig. 5*D*). This suggests that Treg expansion is likely occurring at similar rates as parallel Teff responses. Therefore, Tregs do not likely contribute significantly to the differences in responses induced by DEC-205^+ and $DCIR2^+$ DCs, and neither DC subset in NOD mice is capable of increasing the Treg-to-Teff ratio to skew toward tolerance.

As the loss of T cells after stimulation by $DCIR2^+$ DCs is not due to altered trafficking to sites of endogenous antigen or due to suppression by Tregs, we hypothesized that $DCIR2^+$ DC stimulation may induce T-cell deletion. As measured by caspase activation and mitochondrial potential, $DCIR2^+$ DCs induced more apoptosis in BDC2.5 T cells than DEC-205^+ DCs (Fig. 6*A* and *B*). Therefore, the reduction in T-cell number after $DCIR2^+$ DC stimulation is likely due to an increase in apoptosis. To strengthen this conclusion, we tested whether antigen delivered to $DCIR2^+$ DCs rendered BDC2.5 T cells unable to respond to subsequent stimulus. NOD mice were injected with BDC2.5 $CD4^+$ cells and treated first with either PBS or αDCIR2-BDC. After 10 days, the mice were treated with either αDCIR2-BDC, αCD40, poly(I:C), and LPS to elicit a strong immunogenic response or PBS as a control. Initial treatment of mice with αDCIR2-BDC led to decreased responsiveness to the challenge; T-cell numbers were lower after the challenge in mice pretreated with αDCIR2-BDC, especially in the lymph node (Fig. 6*C*). Therefore, targeting of antigen to $DCIR2^+$ DCs in NOD mice leads to decreased responsiveness that cannot be fully rescued by immunogenic challenge and further suggests increased deletion of T cells after stimulation by αDCIR2-BDC.

To determine what distinct genetic programs are elicited in the T cells early after stimulation by the two DC subsets, we sorted BDC2.5 T cells for gene expression analysis 14 h after stimulation in vivo with either αDEC-BDC or αDCIR2-BDC. We found a set of genes with significant differential expression in BDC2.5 T cells stimulated by the two DC subsets in NOD mice (Fig. 7*A*

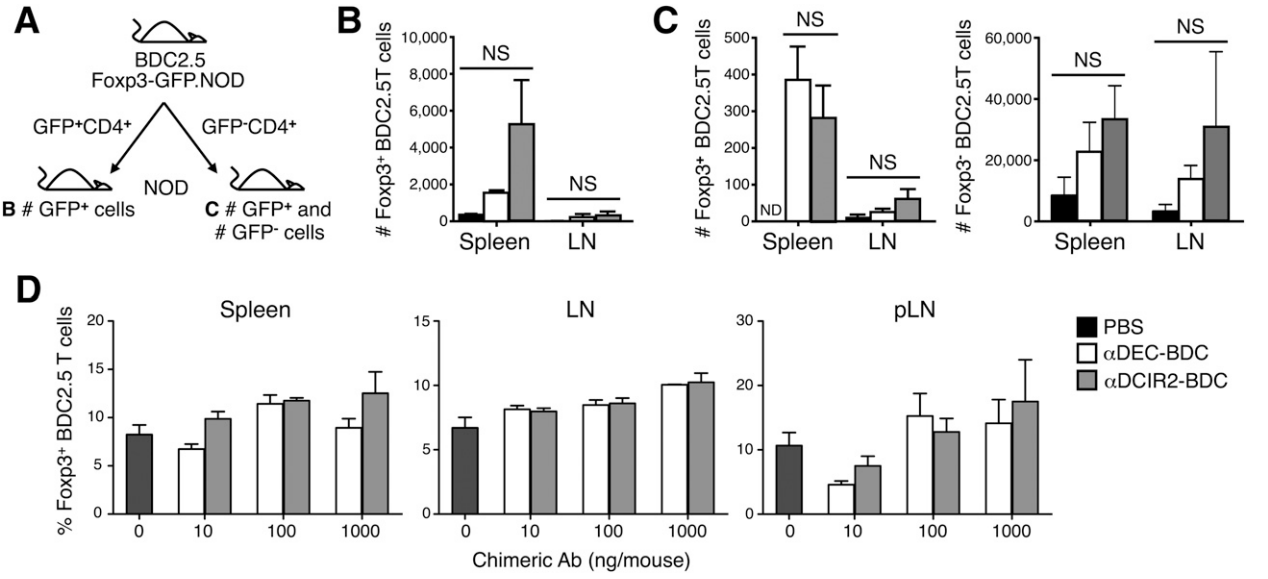

Figure 5—DEC-205^+ and $DCIR2^+$ DCs induce similar Treg proliferation, with little Treg induction and no increase in the Treg-to-Teff ratio. *A*: BDC2.5 $Foxp3^+$ T cells and BDC2.5 $Foxp3^-$ T cells, sorted from BDC2.5.Foxp3-GFP mice, were stimulated in vivo with αDEC-BDC or αDCIR2-BDC for 3 days in NOD mice. *B*: The number of GFP^+ cells was assessed among transferred GFP^+ cells after treatment with the indicated antibodies. Average of three independent experiments ± SEM. *C*: The number of GFP^+ cells converted from transferred GFP^- cells (left) and the number of GFP^- cells (right) expanded by the indicated treatments were assessed. Average of three independent experiments ± SEM. *D*: NOD mice were injected with BDC2.5 T cells, and 5 days after treatment with the indicated antibodies, the total percentage of BDC2.5 T cells expressing Foxp3 was measured. Average of two independent experiments ± SEM. No significant differences were observed by statistical analysis with one-way ANOVA (*B* and *C*) or two-way ANOVA (*D*). LN, lymph nodes; ND, not detected; NS, not significant; pLN, pancreatic lymph nodes.

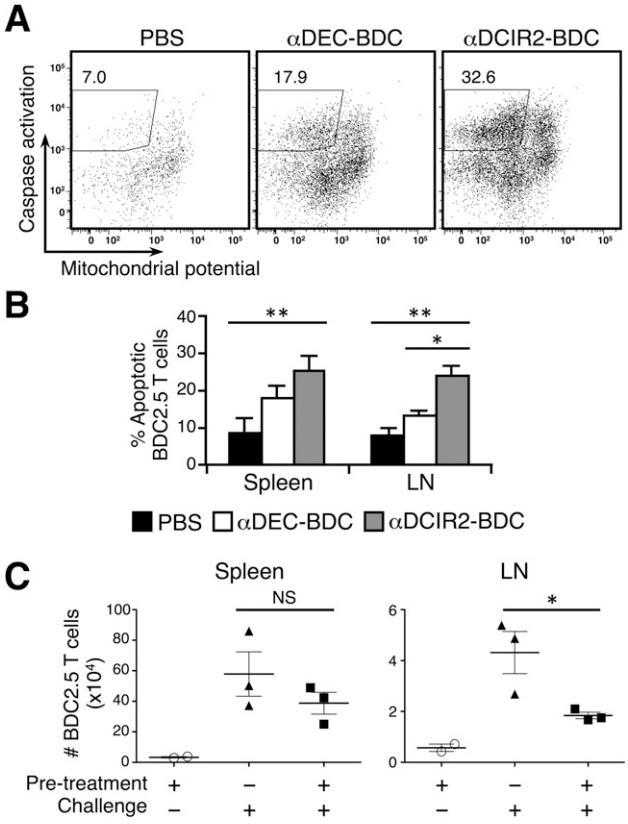

Figure 6—αDCIR2-BDC increases BDC2.5 T-cell apoptosis and decreases responsiveness to antigen rechallenge. *A*: BDC2.5 cells from spleen were assessed for caspase activation and mitochondrial membrane potential after 4 days with the indicated treatments in NOD mice. *B*: The average percentage of BDC2.5 cells within the apoptotic gate in spleen and lymph nodes (LNs). Average of three experiments ± SEM. **P* < 0.05, ***P* < 0.005. *C*: NOD mice injected with BDC2.5 T cells were treated with either PBS or αDCIR2-BDC intraperitoneally. Ten days after the initial treatment, mice were challenged with αDCIR2-BDC + LPS + poly(I:C) + αCD40 or given PBS as a control. Five days later (day 15 after initial treatment), numbers of transferred cells in spleen and LNs were assessed. Each dot represents cells from a single mouse, representative of three individual experiments. Statistical analysis was performed with one-way ANOVA with Bonferroni posttests. **P* < 0.05. NS, not significant.

and Supplementary Table 1). Although both DCs stimulated the T cells, larger gene expression changes occurred with DCIR2$^+$ DC stimulation compared with DEC-205$^+$ DC stimulation (Supplementary Fig. 3). Pathway analysis determined a preferential expression of gene sets related to leukocyte activation (gene ontology ID 45321) in immune system process-related genes (gene ontology ID 2376) in T cells with αDCIR2-BDC stimulation over αDEC-BDC stimulation at this early time point (enrichment score = 8.22) (Fig. 7*B*). The specific leukocyte activation genes with greater than twofold change are shown in Fig. 7*C*. These data give further evidence that the lack of T-cell expansion at later time points is not due to an inability of DCIR2$^+$ DCs to elicit a response via the TCR and suggest instead active tolerance induction. IFN response genes, including *Irf1*, are downregulated more ($P = 9.13 \times 10^{-3}$, fold change −1.70) in T cells after DCIR2$^+$ DC stimulation (Fig. 7*C*), which correlates with the lack of IFN-γ production in DCIR2-stimulated T cells. Matching the observed increased IL-2 protein secretion at day 3 (Fig. 3), T cells stimulated by DCIR2$^+$ DCs expressed more *Il2* message early. In addition, *Il3* message was much higher in DCIR2$^+$ DC-stimulated BDC2.5 T cells compared with DEC-205$^+$ DC-stimulated T cells (Fig. 7*A* and Supplementary Table 1). Quantitative measurement of mRNA levels for *Il2*, *Il3*, and *Irf1* confirmed the different expression observed by microarray (Supplementary Fig. 4*A*). IL-3 protein expression was observed on day 1 after stimulation by DCIR2$^+$ DCs, but not DEC-205$^+$ DCs, but it was gone by day 3 (Supplementary Fig. 4*B* and *C*).

Importantly, expression of the transcription factor *Zbtb32* is upregulated in T cells after αDCIR2-BDC stimulation significantly more compared with αDEC-BDC stimulation ($P = 4.54 \times 10^{-3}$, 3.66-fold change) (Fig. 7*A* and Supplementary Table 1). Quantitative measurement of *Zbtb32* mRNA levels across a wide range of antibody doses confirmed this preferential induction in DCIR2-stimulated T cells (Fig. 8*A*). Higher *Zbtb32* induction was also observed in vitro when BDC2.5 T cells were directly cultured with a BDC2.5-specific peptide and sorted splenic CD11b$^+$ DCs, compared with CD8$^+$ DCs. After 14 h of culture, *Zbtb32* expression was 1.47-fold higher ($P < 0.05$) in sorted T cells stimulated with CD11b$^+$ DCs compared with CD8$^+$ DCs. Zbtb32 is a zinc-finger protein that is induced with activation and has been shown to inhibit CD4$^+$ T-cell differentiation and cytokine production (42–45), which might contribute to the lack of cytokine production observed in αDCIR2-BDC–stimulated T cells. To determine the effect of Zbtb32 on T-cell responses, CD4$^+$ T cells from NOD.BDC2.5 mice were transfected with a plasmid encoding *Zbtb32* or a control plasmid. Transfection efficiency was tested using cotransfection with GFP and Western blotting (Fig. 8*B* and Supplementary Fig. 5*A* and *B*). Although *Zbtb32* transfection did not directly affect viability (Supplementary Fig. 5*A*), overexpression of Zbtb32 reduced expansion and IFN-γ production in BDC2.5 T cells after in vitro stimulation, similar to observed changes after stimulation with DCIR2$^+$ DCs in vivo (Fig. 8*C* and *D*). We next determined the diabetogenicity of BDC2.5 T cells overexpressing Zbtb32 using the NOD.*scid* transfer model. BDC2.5 CD4$^+$ T cells transfected with either *Zbtb32* or control plasmid were transferred to NOD.*scid* mice. Mice that received T cells transfected with *Zbtb32* had significantly delayed diabetes compared with mice that received T cells transfected with the control plasmid (Fig. 8*E*). Insulitis scores at day 6 (before the development of hyperglycemia) were lower in NOD.*scid* mice that received Zbtb32-expressing T cells, and fewer of these cells were recovered in lymphoid tissues, including in the pancreas-draining lymph nodes (Fig. 8*F* and *G*). Hence, Zbtb32 is increased by T-cell interactions with DCIR2$^+$

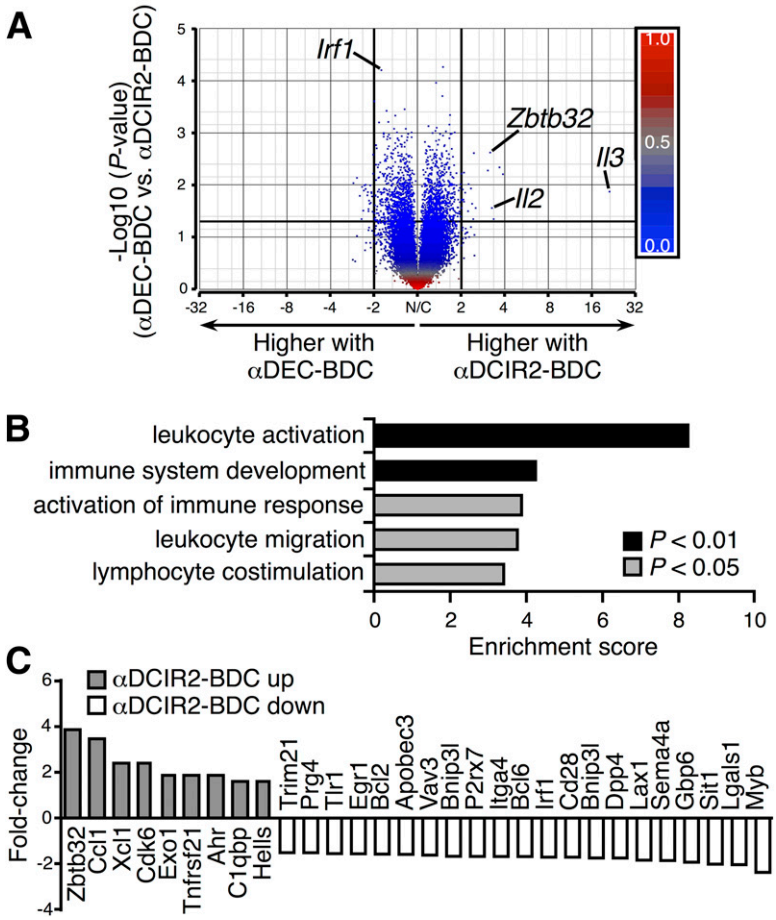

Figure 7—In vivo stimulation with αDCIR2-BDC induces distinct gene expression changes in BDC2.5 T cells. BDC2.5 T cells were transferred to NOD mice, followed by treatment with αDEC-BDC or αDCIR2-BDC. Fourteen hours after treatment, BDC2.5 T cells were sorted from spleen and lymph nodes and RNA was obtained and then analyzed by microarray. Genes differentially regulated by DCIR2$^+$ and DEC-205$^+$ DCs are analyzed by a volcano plot of genes (dark lines indicate a *P* value of 0.05 [horizontal] and a twofold change [vertical]) (*A*) and a pathway analysis of immune system process in gene ontology ID 2376 ($P < 0.05$, false discovery rate < 0.75) (*B*). From the data in *B*, leukocyte activation-related genes are shown in *C* ($P < 0.05$, false discovery rate < 0.75).

DCs, and this transcriptional regulator can inhibit expansion of islet-specific CD4$^+$ T cells and their diabetogenic potential.

DISCUSSION

Taken together, these data demonstrate that DEC-205$^+$ and DCIR2$^+$ DCs in NOD mice stimulate effector and tolerant responses, respectively, in autoreactive CD4$^+$ T cells and have a differential ability to induce diabetes-inhibiting T-cell responses. The observed reduction in T-cell numbers after stimulation by DCIR2$^+$ DCs has several potential mechanisms. First, T cells could possibly expand less due to a lower level of stimulation, but we observed similar levels of early activation marker protein expression and proliferation in BDC2.5 T cells after stimulation with either DC subset. The gene expression signatures actually indicate a stronger activation and proliferative signal in T cells stimulated by DCIR2$^+$ DCs. Second, T cells could be migrating to sites of endogenous antigen expression, yet DCIR2$^+$ DC-stimulated T cells are not preferentially accumulating in the pancreas-draining lymph nodes. Finally, after initial proliferation, T cells stimulated with DCIR2$^+$ DCs may undergo more apoptosis. This third mechanism is consistent with our data that caspase activation is increased, and T cells have lower responsiveness to secondary antigen challenge. Therefore, the increased tolerance induction in T cells after DCIR2$^+$ DC stimulation is likely due to increased deletion. Because DCIR2$^+$ DCs are more abundant in the spleen, and DEC-205$^+$ DCs more abundant in the lymph node, these differences could be due in part to the different initial sites of activation.

In contrast to wild-type mice, neither DEC-205$^+$ nor DCIR2$^+$ DCs are able to induce a net increase in regulatory T cells. Previously, we observed that bone marrow–derived DCs from NOD mice could expand functional Tregs in vitro with IL-2 (46,47). However, our data here show the inability of both of these DC subsets to increase Tregs in vivo in NOD mice. This indicates a second defect in DC-mediated peripheral tolerance in NOD mice and highlights possible differences in the environment in

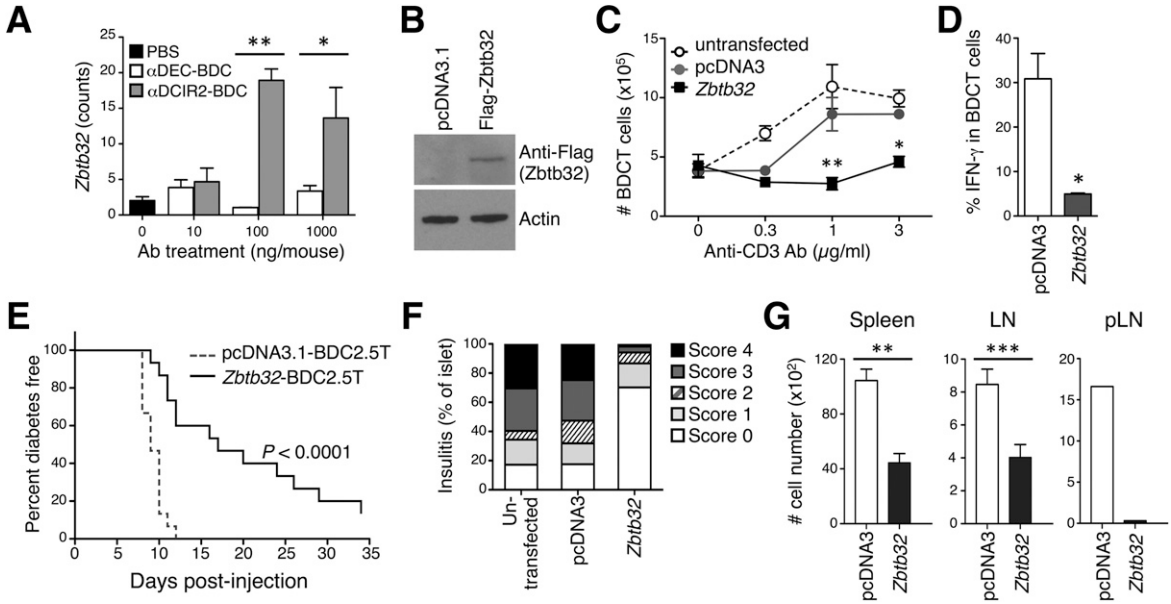

Figure 8—Overexpression of Zbtb32 in BDC2.5 T cells inhibits T-cell expansion, IFN-γ production, and diabetes development. *A*: BDC2.5 T cells were transferred to NOD mice, followed by the indicated treatments. Fourteen hours after treatment, BDC2.5 T cells were sorted from spleen and RNA was obtained and then analyzed by NanoString nCounter analysis. $^{**}P < 0.001$; $^{*}P < 0.05$. *B*: BDC2.5 T cells were transfected with the indicated plasmids and allowed to rest for 14 h before being lysed. Western blotting was performed using anti-Flag antibodies (top), with anti-actin antibodies (bottom) as a loading control. Transfected BDC2.5 T cells were stimulated with the indicated concentration of plate-bound anti-CD3 antibody and anti-CD28 antibody in vitro for 3 days to see the proliferation ($^{**}P < 0.001$, $^{*}P < 0.01$) (*C*) and IFN-γ secretion after the phorbol myristic acid and ionomycin stimulation ($^{*}P < 0.05$) (*D*). *E–G*: BDC2.5 T cells were transfected with the indicated plasmids and transferred to NOD.*scid* mice. *E*: Percent of NOD.*scid* mice that were diabetes free at the indicated time points after BDC2.5 T-cell injection is shown. $P < 0.0001$ ($n = 15$ mice). Six days after T-cell injection, the pancreata were harvested and scored for the degree of insulitis, with at least 20 islets per pancreas analyzed by two independent examiners (*F*), and the numbers of transferred cells in spleen, lymph nodes (LNs), and pLN (pooled from three mice) were assessed (*G*). $^{**}P < 0.01$; $^{***}P = 0.0005$ ($n = 3$ mice). Statistical analysis was performed with two-way ANOVA with Bonferroni posttests (*A* and *C*), Student *t* test (*D* and *G*), and log-rank test (*E*). pLN, pancreatic lymph nodes.

which these DCs act during chronic autoimmunity. DCIR2$^+$ DC stimulation in NOD, although more tolerogenic than NOD DEC-205$^+$ DCs, may not optimally induce tolerance, as diabetes was delayed but not completely abrogated after treatment. Because the DCIR2-induced deletion tolerance is intrinsic to the affected T cells and not dominant tolerance such as that mediated by regulatory T cells, this type of treatment may require delivery of antigen multiple times. Therefore, it will be important to identify signals that create the proper context for therapeutic tolerance induction via DCIR2$^+$ DCs and to determine how to use DCs in vivo to induce dominant tolerance during autoimmunity.

DCIR2$^+$ and DEC-205$^+$ DCs induce distinct genetic programs in autoreactive T cells early after activation that correlate with the differential T-cell phenotypes observed, including decreased *Irf1* expression that correlates with decreased IFN-γ production. High IL-3 expression is also induced early after DCIR2$^+$ DC stimulation. Interestingly, IL-3 therapy can block diabetes development in NOD mice, suggesting that, in some contexts, IL-3 may be an important regulator of autoimmunity (48,49). It also presents the possibility that these two DC subsets may induce T-cell tolerance through different pathways, some of which are likely impaired in NOD mice. At the transcriptional level, we observed higher *Zbtb32* in T cells stimulated by DCIR2$^+$ DCs. T cells overexpressing Zbtb32 displayed an inhibited ability to transfer diabetes, demonstrating that Zbtb32 is an important cell-intrinsic regulator of T-cell tolerance. Zbtb32 is a known negative regulator of cytokine production (33) and correlates with nuclear factor of activated T-cells–mediated T-cell nonresponsiveness (50). Our data suggest Zbtb32 may also regulate antigen-induced cell death.

Our data point to two possible therapeutic targets: utilizing cDC2 DCIR2$^+$ DCs to induce tolerance and generating tolerance in T cells by upregulating Zbtb32. For optimal in vivo tolerance induction, the inflammatory environment in which DCs stimulate T cells during chronic autoimmunity also needs to be addressed. In conclusion, this study indicates that to preferentially elicit the desired tolerogenic response, antigen-specific treatment of type 1 diabetes and other autoimmune diseases will need to target antigen to the correct DC subset to present antigen to autoreactive T cells.

Acknowledgments. The authors thank Alice Franks (DEOB, NIDDK) for mouse husbandry, the National Heart, Lung, and Blood Institute/NIDDK flow core for sorting, Amiran K. Dzutsev (National Cancer Institute [NCI]) for helping with the design of NanoString analysis, Patricia Johnson and Steve Shema (CCR

Genomics Core, NCI) for technical support with NanoString analysis, and Weiping Chen and Chithra Keembiyehetty (NIDDK Genomics Core) for gene array support.

Funding. This work was supported by the Division of Intramural Research, NIDDK, and JDRF.

Duality of Interest. No potential conflicts of interest relevant to this article were reported.

Author Contributions. J.D.P. designed the project, collected and analyzed data, and wrote the manuscript. C.H.-I. designed the project, collected and analyzed data, and revised the manuscript. Y.Z. provided reagents and collected and analyzed data. N.M.B. collected and analyzed data. K.V.T. designed the project, analyzed data, and wrote the manuscript. K.V.T. is the guarantor of this work and, as such, had full access to all the data in the study and takes responsibility for the integrity of the data and the accuracy of the data analysis.

References

1. Bluestone JA, Herold K, Eisenbarth G. Genetics, pathogenesis and clinical interventions in type 1 diabetes. Nature 2010;464:1293–1300
2. Clemente-Casares X, Tsai S, Huang C, Santamaria P. Antigen-specific therapeutic approaches in type 1 diabetes. Cold Spring Harb Perspect Med 2012; 2:a007773
3. Ben-Nun A, Kaushansky N, Kawakami N, et al. From classic to spontaneous and humanized models of multiple sclerosis: Impact on understanding pathogenesis and drug development. J Autoimmun 2014;54:33–50
4. Jayasimhan A, Mansour KP, Slattery RM. Advances in our understanding of the pathophysiology of type 1 diabetes: lessons from the NOD mouse. Clin Sci (Lond) 2014;126:1–18
5. Price JD, Tarbell KV. The role of dendritic cell subsets and innate immunity in the pathogenesis of type 1 diabetes and other autoimmune diseases [article online], 2015. Front Immunol. Available from http://dx.doi.org/10.3389/fimmu.2015.00288. Accessed 15 June 2015
6. Welzen-Coppens JM, van Helden-Meeuwsen CG, Leenen PJ, Drexhage HA, Versnel MA. Reduced numbers of dendritic cells with a tolerogenic phenotype in the prediabetic pancreas of NOD mice. J Leukoc Biol 2012;92:1207–1213
7. Calderon B, Carrero JA, Miller MJ, Unanue ER. Cellular and molecular events in the localization of diabetogenic T cells to islets of Langerhans. Proc Natl Acad Sci U S A 2011;108:1561–1566
8. Morel PA. Dendritic cell subsets in type 1 diabetes: friend or foe? Front Immunol 2013;4:415
9. Turley SJ. Dendritic cells: inciting and inhibiting autoimmunity. Curr Opin Immunol 2002;14:765–770
10. Guilliams M, Ginhoux F, Jakubzick C, et al. Dendritic cells, monocytes and macrophages: a unified nomenclature based on ontogeny. Nat Rev Immunol 2014;14:571–578
11. Bachem A, Güttler S, Hartung E, et al. Superior antigen cross-presentation and XCR1 expression define human CD11c+CD141+ cells as homologues of mouse CD8+ dendritic cells. J Exp Med 2010;207:1273–1281
12. Hildner K, Edelson BT, Purtha WE, et al. Batf3 deficiency reveals a critical role for CD8alpha+ dendritic cells in cytotoxic T cell immunity. Science 2008; 322:1097–1100
13. Iyoda T, Shimoyama S, Liu K, et al. The CD8+ dendritic cell subset selectively endocytoses dying cells in culture and in vivo. J Exp Med 2002;195: 1289–1302
14. Liu K, Iyoda T, Saternus M, Kimura Y, Inaba K, Steinman RM. Immune tolerance after delivery of dying cells to dendritic cells in situ. J Exp Med 2002; 196:1091–1097
15. Ferris ST, Carrero JA, Mohan JF, Calderon B, Murphy KM, Unanue ER. A minor subset of Batf3-dependent antigen-presenting cells in islets of Langerhans is essential for the development of autoimmune diabetes. Immunity 2014;41:657–669
16. Jeker LT, Bour-Jordan H, Bluestone JA. Breakdown in peripheral tolerance in type 1 diabetes in mice and humans. Cold Spring Harb Perspect Med 2012;2: a007807
17. Jansen A, van Hagen M, Drexhage HA. Defective maturation and function of antigen-presenting cells in type 1 diabetes. Lancet 1995;345:491–492
18. Price JD, Beauchamp NM, Rahir G, et al. CD8+ dendritic cell-mediated tolerance of autoreactive CD4+ T cells is deficient in NOD mice and can be corrected by blocking CD40L. J Leukoc Biol 2014;95:325–336
19. Steptoe RJ, Ritchie JM, Harrison LC. Increased generation of dendritic cells from myeloid progenitors in autoimmune-prone nonobese diabetic mice. J Immunol 2002;168:5032–5041
20. Judkowski V, Pinilla C, Schroder K, Tucker L, Sarvetnick N, Wilson DB. Identification of MHC class II-restricted peptide ligands, including a glutamic acid decarboxylase 65 sequence, that stimulate diabetogenic T cells from transgenic BDC2.5 nonobese diabetic mice. J Immunol 2001;166:908–917
21. Haskins K, Portas M, Bergman B, Lafferty K, Bradley B. Pancreatic islet-specific T-cell clones from nonobese diabetic mice. Proc Natl Acad Sci U S A 1989;86:8000–8004
22. Stadinski BD, Delong T, Reisdorph N, et al. Chromogranin A is an autoantigen in type 1 diabetes. Nat Immunol 2010;11:225–231
23. Feuerer M, Shen Y, Littman DR, Benoist C, Mathis D. How punctual ablation of regulatory T cells unleashes an autoimmune lesion within the pancreatic islets. Immunity 2009;31:654–664
24. Tang Q, Adams JY, Penaranda C, et al. Central role of defective interleukin-2 production in the triggering of islet autoimmune destruction. Immunity 2008;28: 687–697
25. Spencer J, Peakman M. Post-mortem analysis of islet pathology in type 1 diabetes illuminates the life and death of the beta cell. Clin Exp Immunol 2009; 155:125–127
26. Fu W, Wojtkiewicz G, Weissleder R, Benoist C, Mathis D. Early window of diabetes determinism in NOD mice, dependent on the complement receptor CRIg, identified by noninvasive imaging. Nat Immunol 2012;13:361–368
27. Lebastchi J, Herold KC. Immunologic and metabolic biomarkers of β-cell destruction in the diagnosis of type 1 diabetes. Cold Spring Harb Perspect Med 2012;2:a007708
28. Sosenko JM, Palmer JP, Greenbaum CJ, et al.; Diabetes Prevention Trial-Type 1 Study Group. Increasing the accuracy of oral glucose tolerance testing and extending its application to individuals with normal glucose tolerance for the prediction of type 1 diabetes: the Diabetes Prevention Trial-Type 1. Diabetes Care 2007;30:38–42
29. Hawiger D, Inaba K, Dorsett Y, et al. Dendritic cells induce peripheral T cell unresponsiveness under steady state conditions in vivo. J Exp Med 2001;194: 769–779
30. Bonifaz L, Bonnyay D, Mahnke K, Rivera M, Nussenzweig MC, Steinman RM. Efficient targeting of protein antigen to the dendritic cell receptor DEC-205 in the steady state leads to antigen presentation on major histocompatibility complex class I products and peripheral CD8+ T cell tolerance. J Exp Med 2002; 196:1627–1638
31. Dudziak D, Kamphorst AO, Heidkamp GF, et al. Differential antigen processing by dendritic cell subsets in vivo. Science 2007;315:107–111
32. Kamphorst AO, Guermonprez P, Dudziak D, Nussenzweig MC. Route of antigen uptake differentially impacts presentation by dendritic cells and activated monocytes. J Immunol 2010;185:3426–3435
33. Bruder D, Westendorf AM, Hansen W, et al. On the edge of autoimmunity: T-cell stimulation by steady-state dendritic cells prevents autoimmune diabetes. Diabetes 2005;54:3395–3401
34. Idoyaga J, Fiorese C, Zbytnuik L, et al. Specialized role of migratory dendritic cells in peripheral tolerance induction. J Clin Invest 2013;123:844–854
35. Neubert K, Lehmann CH, Heger L, et al. Antigen delivery to CD11c+CD8- dendritic cells induces protective immune responses against experimental melanoma in mice in vivo. J Immunol 2014;192:5830–5838
36. Zang YS, Fang Z, Liu YA, Li B, Xiu QY. Repressor of GATA-3 can negatively regulate the expression of T cell cytokines through modulation on inducible costimulator. Chin Med J (Engl) 2012;125:2188–2194

37. Clynes RA, Towers TL, Presta LG, Ravetch JV. Inhibitory Fc receptors modulate in vivo cytotoxicity against tumor targets. Nat Med 2000;6:443–446
38. Gardner JM, Metzger TC, McMahon EJ, et al. Extrathymic Aire-expressing cells are a distinct bone marrow-derived population that induce functional inactivation of CD4+ T cells. Immunity 2013;39:560–572
39. Skokos D, Shakhar G, Varma R, et al. Peptide-MHC potency governs dynamic interactions between T cells and dendritic cells in lymph nodes. Nat Immunol 2007;8:835–844
40. Haskins K, Cooke A. CD4 T cells and their antigens in the pathogenesis of autoimmune diabetes. Curr Opin Immunol 2011;23:739–745
41. Yamazaki S, Dudziak D, Heidkamp GF, et al. CD8+ CD205+ splenic dendritic cells are specialized to induce Foxp3+ regulatory T cells. J Immunol 2008; 181:6923–6933
42. Hirahara K, Yamashita M, Iwamura C, et al. Repressor of GATA regulates TH2-driven allergic airway inflammation and airway hyperresponsiveness. J Allergy Clin Immunol 2008;122:512.e11–520.e11
43. Yoon HS, Scharer CD, Majumder P, et al. ZBTB32 is an early repressor of the CIITA and MHC class II gene expression during B cell differentiation to plasma cells. J Immunol 2012;189:2393–2403
44. Beaulieu AM, Zawislak CL, Nakayama T, Sun JC. The transcription factor Zbtb32 controls the proliferative burst of virus-specific natural killer cells responding to infection. Nat Immunol 2014;15:546–553
45. Miaw SC, Kang BY, White IA, Ho IC. A repressor of GATA-mediated negative feedback mechanism of T cell activation. J Immunol 2004;172:170–177
46. Tarbell KV, Yamazaki S, Olson K, Toy P, Steinman RM. CD25+ CD4+ T cells, expanded with dendritic cells presenting a single autoantigenic peptide, suppress autoimmune diabetes. J Exp Med 2004;199:1467–1477
47. Tarbell KV, Petit L, Zuo X, et al. Dendritic cell-expanded, islet-specific CD4+ CD25+ CD62L+ regulatory T cells restore normoglycemia in diabetic NOD mice. J Exp Med 2007;204:191–201
48. Enzler T, Gillessen S, Dougan M, et al. Functional deficiencies of granulocyte-macrophage colony stimulating factor and interleukin-3 contribute to insulitis and destruction of beta cells. Blood 2007;110:954–961
49. Ito A, Aoyanagi N, Maki T. Regulation of autoimmune diabetes by interleukin 3-dependent bone marrow-derived cells in NOD mice. J Autoimmun 1997;10: 331–338
50. Martinez GJ, Pereira RM, Äijö T, et al. The transcription factor NFAT promotes exhaustion of activated CD8+ T cells. Immunity 2015;42:265–278